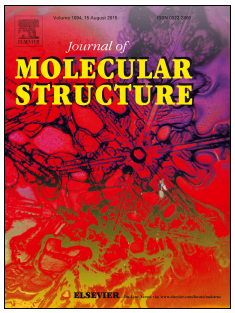

Synthesis, X-ray structure, Hirshfeld analysis, and DFT studies of a new Pd(II) complex with an anionic *s*-triazine *NNO* donor ligand

Saied M. Soliman, Jamal Lasri, Matti Haukka, Adel Elmarghany, Abdullah Mohammed Al-Majid, Ayman El-Faham, Assem Barakat

PII: S0022-2860(20)30788-2

DOI: https://doi.org/10.1016/j.molstruc.2020.128463

Reference: MOLSTR 128463

To appear in: *Journal of Molecular Structure*

Received Date: 12 March 2020

Revised Date: 7 May 2020

Accepted Date: 14 May 2020

Please cite this article as: S.M. Soliman, J. Lasri, M. Haukka, A. Elmarghany, A.M. Al-Majid, A. El-Faham, A. Barakat, Synthesis, X-ray structure, Hirshfeld analysis, and DFT studies of a new Pd(II) complex with an anionic *s*-triazine *NNO* donor ligand, *Journal of Molecular Structure* (2020), doi: https://doi.org/10.1016/j.molstruc.2020.128463.

Synthesis, X-ray structure, Hirshfeld analysis, and DFT studies of a new Pd(II) complex with an anionic *s*-triazine *NNO* donor ligand

Saied M. Soliman[1]*, Jamal Lasri[2]*, Matti Haukka[3], Adel Elmarghany[4,5], Abdullah Mohammed Al-Majid,[4] Ayman El-Faham[1,4], and Assem Barakat[4]*

[1]Department of Chemistry, Faculty of Science, Alexandria University, P.O. Box 426, Ibrahimia, Alexandria 21321, Egypt

[2]Department of Chemistry, Rabigh College of Science and Arts, P.O. Box 344, King Abdulaziz University, Jeddah, Saudi Arabia

[3]Department of Chemistry, University of Jyväskylä, P.O. Box 35, FI-40014 Jyväskylä, Finland

[4]Department of Chemistry, College of Science, King Saud University, P.O. Box 2455, Riyadh 11451, Saudi Arabia

[5]Chemistry Department, Faculty of Science, Suez Canal University, Ismailia 41522, Egypt

***** Correspondence: Saied M. Soliman: saied1soliman@yahoo.com (S.M.S.); Jamal Lasri: jlasri@kau.edu.sa (J.L.); Assem Barakat: ambarakat@ksu.edu.sa (A.B.).

Abstract

A new Pd(II) complex, **[Pd(Triaz)Cl]**, with the hydrazono-*s*-triazine ligand, 2,4-di-*tert*-butyl-6-((2-(4-morpholino-6-(phenylamino)-1,3,5-triazin-2-yl)hydrazono)methyl)phenol, was synthesized by the reaction of $PdCl_2$ with the organic ligand (1:1) in acetone under isothermal conditions. The molecular structure of the **[Pd(Triaz)Cl]** complex was determined using FTIR and ^{1}H NMR spectroscopic techniques, and single-crystal X-ray diffraction. Moreover, using Hirshfeld surface analysis, the percentages of the intermolecular interactions were determined. The obtained values were 60.6%, 11.6%, 8.1%, 3.6%, and 5.0% for the H···H, C···H, O···H, N···H, and Cl···H interactions, respectively. Among them, the O···H, C···H and C···Ninteractions are considered extremely important. Natural bond orbital calculations have been used to calculate the amount of electron transfer from the ligand to the metal ion and to evaluate the Pd-N, Pd-O, and Pd-Cl coordination bonding interactions.

Keywords: *S*-triazine; Hydrazone; Pd(II) complex; Hirshfeld surface analysis; NBO

Introduction

s-Triazine is a heterocyclic motif for multiple synthetic and natural products [1]. Being an important scaffold, *s*-triazine derivatives have been extensively studied in both pharmaceutical and coordination chemistry [2,3]. Some of these derivatives, e.g., 2-amino-4-morphlino-*s*-triazine, and hexamethylmelamine, exhibited a wide range of pharmaceutical features such as antitumor activity [4], antioxidant [5], antiviral [6], herbicidal, antimicrobial, and antibacterial [7] properties. Furthermore, the syntheses of various mono-, di-, and tri-substituted *s*-triazines derivatives from cyanuric chloride have been reported-with remarkable pharmaceutical activities [8-13] In particular, hydrazine-based *s*-triazines derivatives have shown potency activities as anticancer agents for A431 (epidermoid carcinoma) and A549 (lung carcinoma) compared to Lapatinib, HKI-272, and AST-1306 as standard references [14]. In addition, they have been used as inhibitors for wtEGFR, EGFR, and mTOR receptors [15,16].

Recently, our research group has reported several complexes bearing *NNN*-tridentate ligands derived from *s*-triazine with divalent metal ions, such as Co(II) [17], Ni(II) [18], Cd(II) [19a] and Mn(II) [19b]. Furthermore, *s*-triazine ligands have been used for recovering Pd(II) from strongly acidic solutions [20].

In this work, we studied the structural aspects of a new Pd(II) complex, **[Pd(Triaz)Cl]**, which contains the hydrazono-*s*-triazine ligand (HTriaz) 2,4-di-*tert*-butyl-6-((2-(4-morpholino-6-(phenylamino)-1,3,5-triazin-2-yl)hydrazono)methyl)phenol (**Scheme 1**). Both molecular and supramolecular structures were investigated using X-ray crystallography, FTIR ^{1}H NMR spectra, Hirshfeld surface analysis, and DFT calculations. The anti-cancer activity was also explored against two cancer cell lines including breast cancer (MCF-7) and human prostate cancer (PC3).

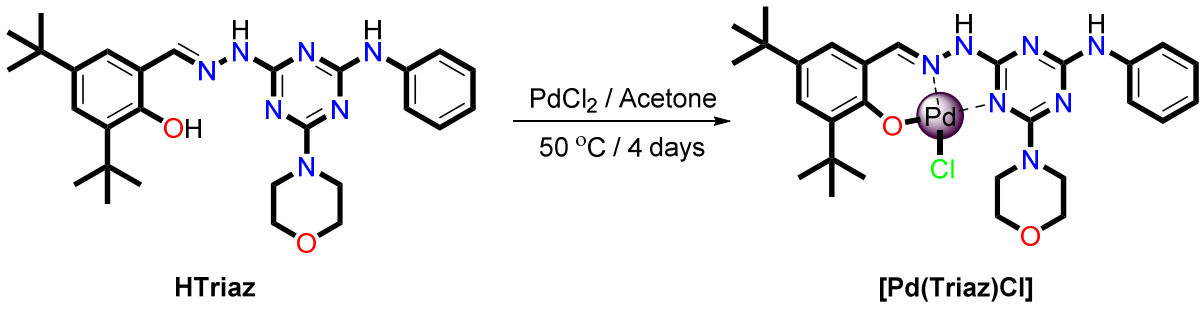

Scheme 1. Synthesis of the **[Pd(Triaz)Cl]** complex.

Experimental

General

FTIR spectra were measured on a PerkinElmer Spectrum 100 FT-IR spectrophotometer (PerkinElmer Inc., Waltham, MA, USA). ^{1}H NMR spectra of **HTriaz** and **[Pd(Triaz)Cl]** were recorded on DMSO-d_6 using a JEOL 400 MHz spectrometer (JEOL Ltd., Tokyo, Japan) at room temperature. Mass spectra were recorded on JMS-600 H JEOL spectrometer (JEOL Ltd., Tokyo, Japan).

Synthesis of the ligand (*E*)-2,4-di-*tert*-butyl-6-((2-(4-morpholino-6-(phenylamino)-1,3,5-triazin-2-yl)hydrazono)methyl)phenol (HTriaz)

The ligand (**HTriaz**) was prepared as previously reported [21].

Synthesis of [Pd(Triaz)Cl] complex

Palladium(II) chloride (21.1 mg, 0.119 mmol) was added to 20 mL of an acetone solution of (**HTriaz**) (60.0 mg, 0.119 mmol). The reaction mixture was stirred at 50 °C for 4 days. Afterwards, the mixture was filtered and maintained at room temperature to allow for the slow evaporation of the solvent, yielding the final product **[Pd(Triaz)Cl]** as reddish-brown block crystals.

^{1}H NMR (400 MHz, DMSO-d_6, ppm): δ 10.84 (s, 1H, N*H*), 8.22 (s, 1H, N*H*), 7.97 (s, 1H, C*H*=N), 7.60 (d, 2H, J_{HH} = 8.1 Hz, phenyl), 7.39 (t, 2H, J_{HH} = 7.6 Hz, phenyl), 7.30 (s, 1H, C_6H_2), 7.22 (s, 1H, C_6H_2), 7.13 (t, 1H, J_{HH} = 7.6 Hz, phenyl), 3.74 (d, 4H, J_{HH} = 4.5 Hz,

morpholine), 3.68 (d, 4H, J_{HH} = 5.0 Hz, morpholine), 1.37 (s, 9H, *tert*-butyl), 1.26 (s, 9H, *tert*-butyl). IR (KBr) cm^{-1}: 3435 (NH), 3263, 3102, 2956, 2856, and 1626 (C=N), and 1579 (C=C). LC-MS (ESI^+-MS): 627.43 $[M]^+$. Anal. calcd. for $C_{28}H_{36}ClN_7O_2Pd$: C, 52.18; H, 5.63; N, 15.21. Found: C, 52.15; H, 5.59; N, 15.25.

X-Ray structural determinations

The crystal of **[Pd(Triaz)Cl]** was immersed in cryo-oil, mounted in a loop, and measured at 170 K. XRD data were collected on a Bruker Kappa Apex II diffractometer with MoKα radiation. For cell refinement and data reduction, the *Denzo-Scalepack* [22] software package was used. A numerical absorption correction (*SADABS* [23]) was applied to the data before structure solution. The structure of **[Pd(Triaz)Cl]** was solved by intrinsic phasing using the SHELXT software [24]. Structural refinement was then performed using the SHELXL-2017 package [24] and the *SHELXLE* [25] graphical user interface. A disordered acetone molecule of as solvent of crystallization in **[Pd(Triaz)Cl]** was disordered over two sites sharing locations of C28 and C28B carbon atoms. The occupancy ratio of the disordered components was 0.51/0.49. The NH hydrogen atoms were located from the difference Fourier map and isotropically refined. The rest of the hydrogen atoms were geometrically positioned and constrained to ride on their parent atoms with C-H = 0.95–0.99 Å and U_{iso} = 1.2–1.5$_{eq}$ (parent atom). Topology analyses were performed using the Crystal Explorer 17.5 program [26] to determine the contribution percentages of the different intermolecular interactions in the crystal structure of **[Pd(Triaz)Cl]**.

Computational details

Density functional theory (DFT) single point calculations were performed using the Gaussian 09 software package [27] with the MPW1PW91 and Wb97XD methods [28] combined with the cc-PVTZ and cc-PVTZ-PP [29] basis sets for nonmetal atoms and Pd, respectively. The multiplicity of the system was set to be 1 because the well known fact that tetra-coordinated

Pd(II) complexes are square planar and diamagnetic. The natural charge populations and interaction energies between the donor atoms and the central metal ion, Pd(II), were computed using NBO 3.1 [30] program.

Results and discussion

Synthesis and characterization of [Pd(Triaz)Cl]

The Pd(II) complex, **[Pd(Triaz)Cl]**, was synthesized as shown in **Scheme 1** and characterized by FTIR, and ^{1}H NMR spectroscopy, ESI^{+}-MS, elemental analysis, and single crystal X-ray diffraction.

The FTIR spectrum of the Pd(II) complex **[Pd(Triaz)Cl]** exhibits signals characteristic for the functional groups as follow: NH (3435), C=N (1628), and C=C (1579 cm^{-1}). In the ^{1}H NMR spectrum, the five phenyl protons were observed as doublet, triplet, and triplet at δ 7.60, 7.39, and 7.13 ppm with coupling constants (J_{HH}) of 8.1, 7.6, and 7.6 Hz (integrations 2:2:1), respectively. Furthermore, the two protons of the tetra substituted phenyl ring (C_6H_2) were observed as two singlets at δ 7.30 and 7.22 ppm. The eight morpholine protons were then detected as doublets at δ 3.74 and 3.68 ppm with coupling constants (J_{HH}) of 4.5 and 5.0 Hz, respectively. The signals of the two *tert*-butyl groups were detected as singlets at δ 1.37 and 1.26 ppm. The two N*H* protons, which appeared at δ 11.30 and 9.34 ppm in the (**HTriaz**) ligand, were slightly shifted in the Pd(II) complex to δ 10.84 and 8.22 ppm. The C*H*=N proton was observed at δ 8.28 ppm in (**HTriaz**); however, it was detected at δ 7.97 ppm in the Pd(II) complex (**Figs. 1–3**).

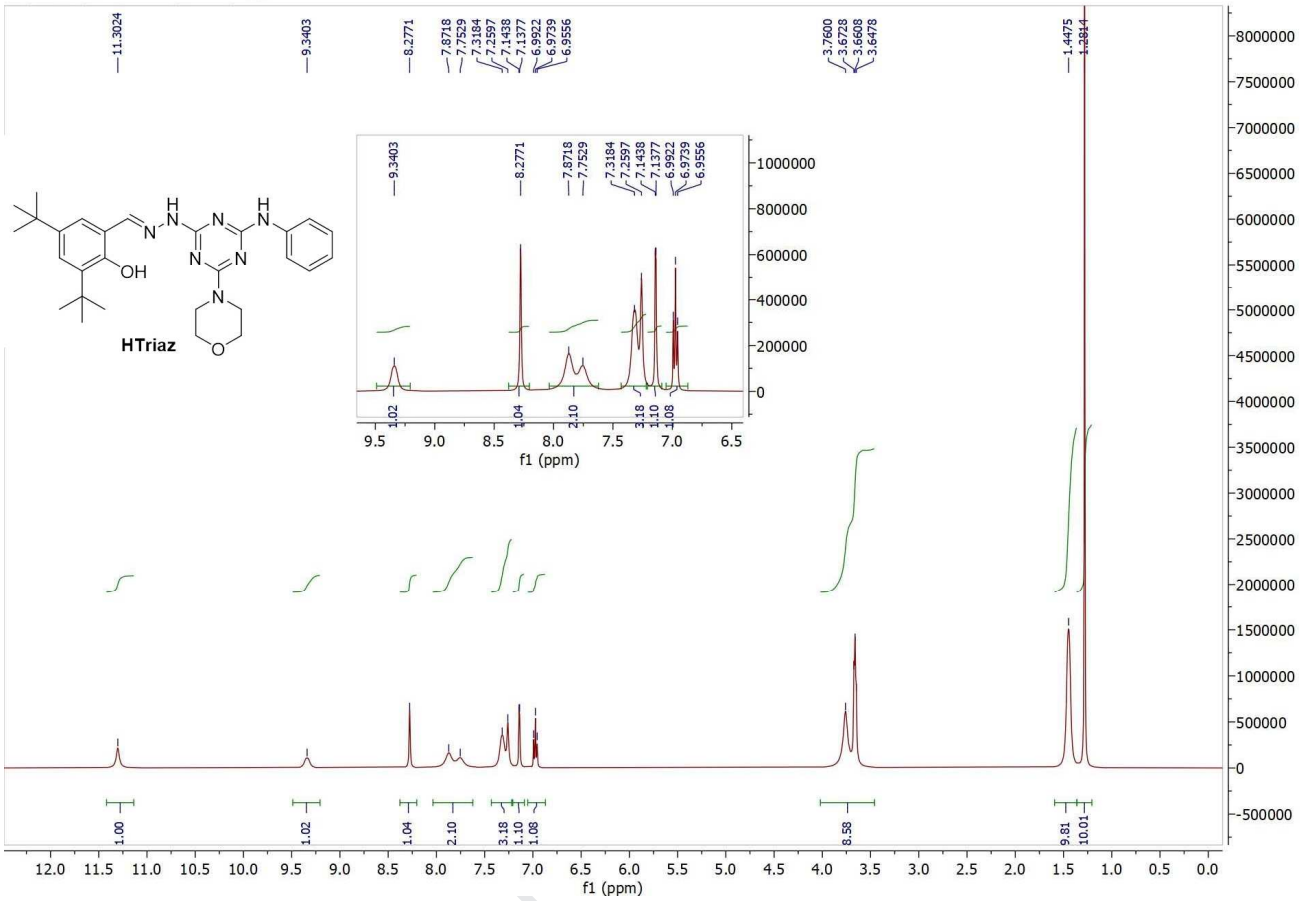

Fig. 1. ^{1}H NMR spectrum of the (**HTriaz**) ligand in DMSO-d_6.

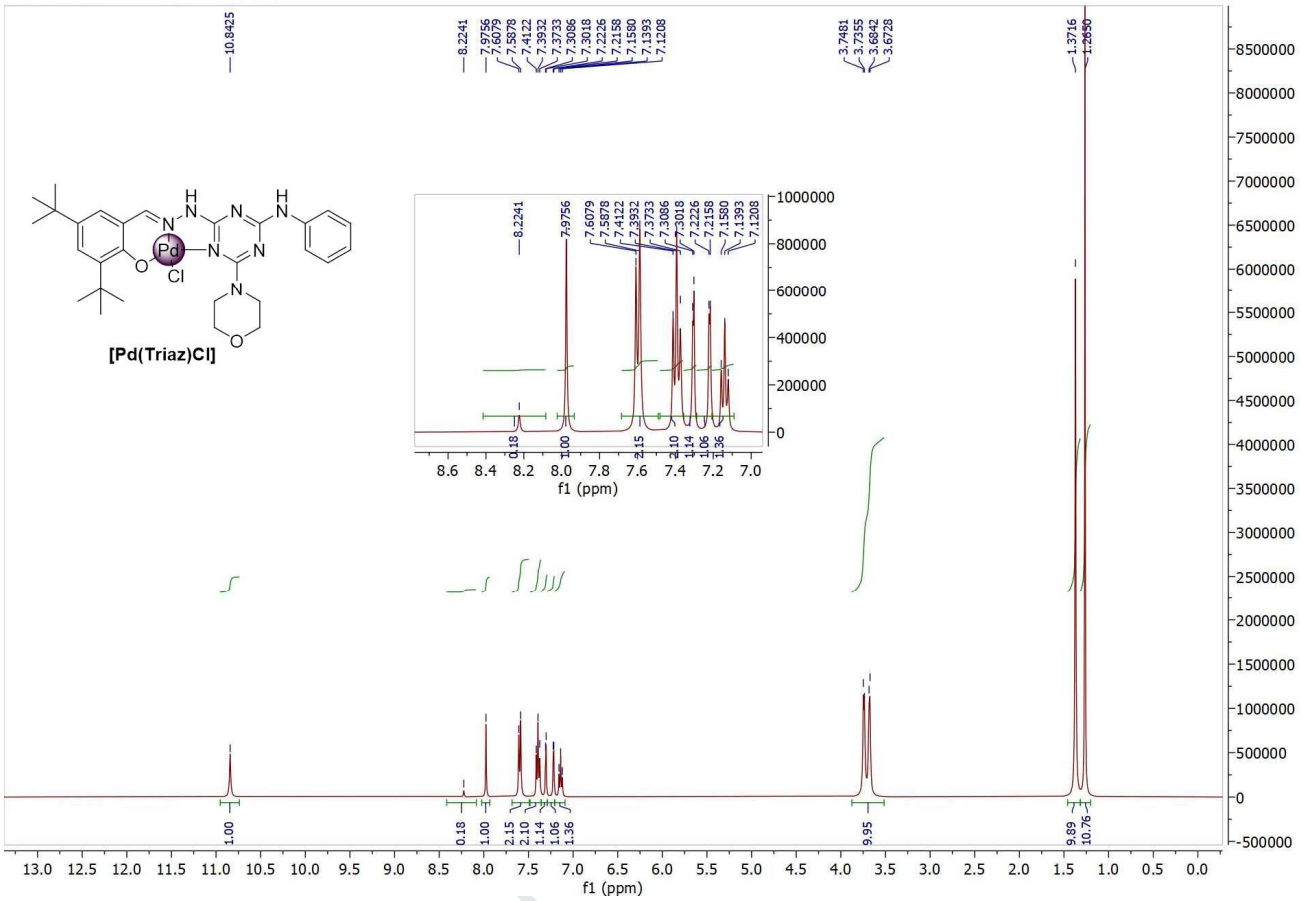

Fig. 2. ^{1}H NMR spectrum of the **[Pd(Triaz)Cl]** complex in DMSO-d_6.

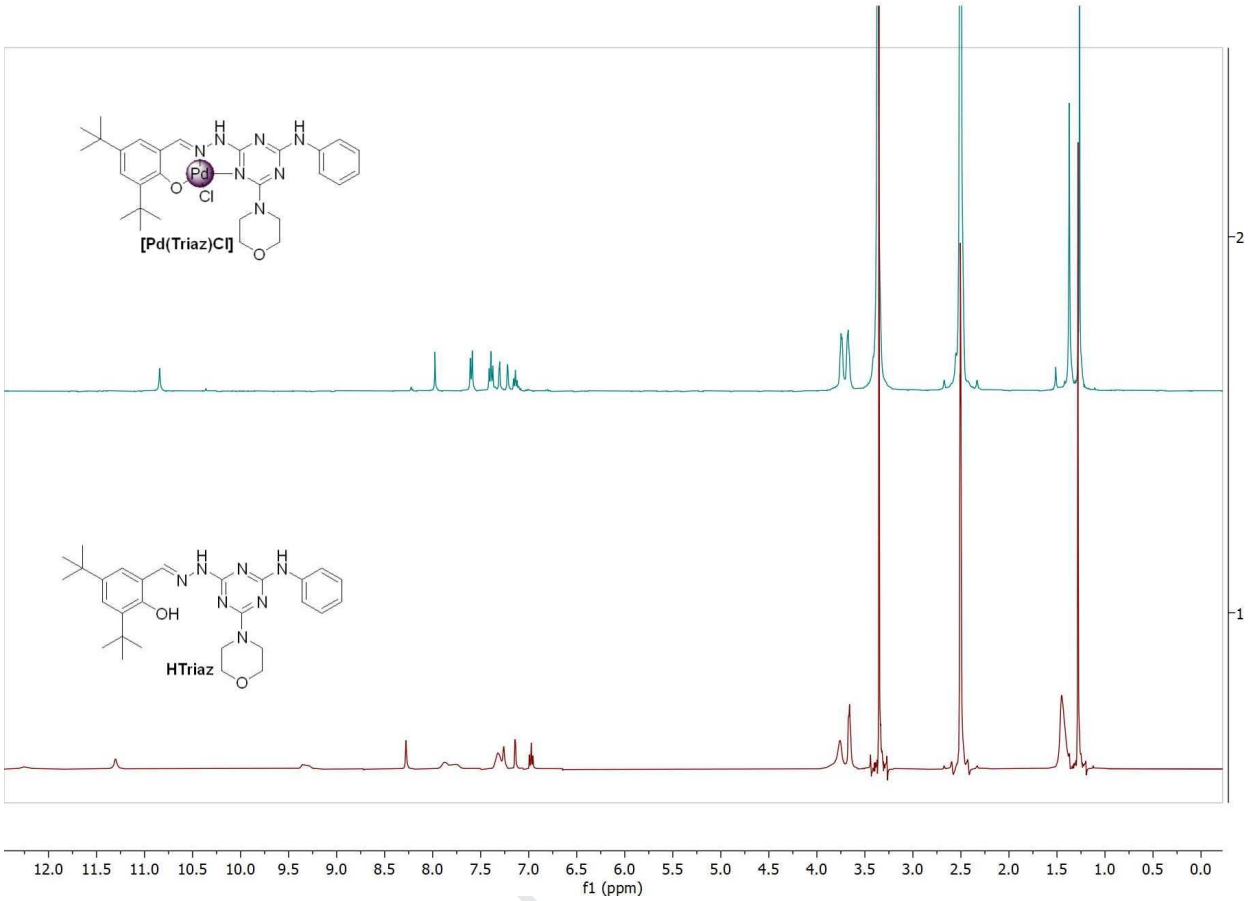

Fig. 3. ^{1}H NMR spectra of (**HTriaz**) and **[Pd(Triaz)Cl]** in DMSO-d_6.

Crystal structure

Fig. 4 shows the X-ray structure of the **[Pd(Triaz)Cl]** complex that crystallized in the monoclinic crystal system and C2/c space group with one molecular unit in the asymmetric unit and Z=8 (**Table 1**). The deprotonated *s*-triazine ligand (**Triaz**$^{-}$) acted as a mononegative *NNO*-donor tridentate chelate coordinating with Pd(II) ion *via* one nitrogen from the *s*-triazine core, one nitrogen from the hydrazone moiety, and the phenolic oxygen atom. The distances between the Pd and donor atoms are 2.054(3), 1.948(3), and 1.964(2) Å for the Pd1-N1, Pd1-N7, and Pd1-O1 bonds, respectively. The coordination sphere of this complex is completed by one chloride ion located *trans* to the N7 atom with a Pd1-Cl1 distance of 2.3270(11) Å. The bite angles of the organic ligand are 80.78°(12) and 91.81°(11) for N7-Pd1-N1 and N7-Pd1-O1, respectively. **Table 2** provides a list of the most important distances

and angles. The angle between the *cis* bonds are in the range of 80.78(12) to 102.14(9)° for the N7-Pd1-N1 and N1-Pd1-Cl1, respectively; and the angles of the *trans* O1-Pd1-N1 and N7-Pd1-Cl1 bonds are 172.46(11) and 177.08(9)°, respectively. The coordination geometry of the Pd(II) ion is considered to be distorted square planar.

Table 1. Crystallographic data of **[Pd(Triaz)Cl]**.

CCDC	1989545
Empirical formula	$C_{31}H_{42}ClN_7O_3Pd$
Fw	702.56
Temp (K)	170(2)
λ (Å)	0.71073
Crystal system	Monoclinic
Space group	C2/c
a (Å)	34.4695(9)
b (Å)	10.1613(3)
c (Å)	22.4498(6)
β (deg)	122.8340(10)
V (Å^3)	6607.0(3)
Z	8
ρ_{calc} (Mg/m^3)	1.413
μ (MoKα) (mm^{-1})	0.685
No. reflns.	45096
Unique reflns.	7566
GOOF (F^2)	1.086
R_{int}	0.0749
R1[a] ($I \geq 2\sigma$)	0.0528
wR2[b] ($I \geq 2\sigma$)	0.0880

[a] $R1 = \Sigma||F_o|-|F_c||/\Sigma|F_o|$. [b] $wR2 = [\Sigma[w(F_o^2-F_c^2)^2]/\Sigma[w(F_o^2)^2]]^{1/2}$.

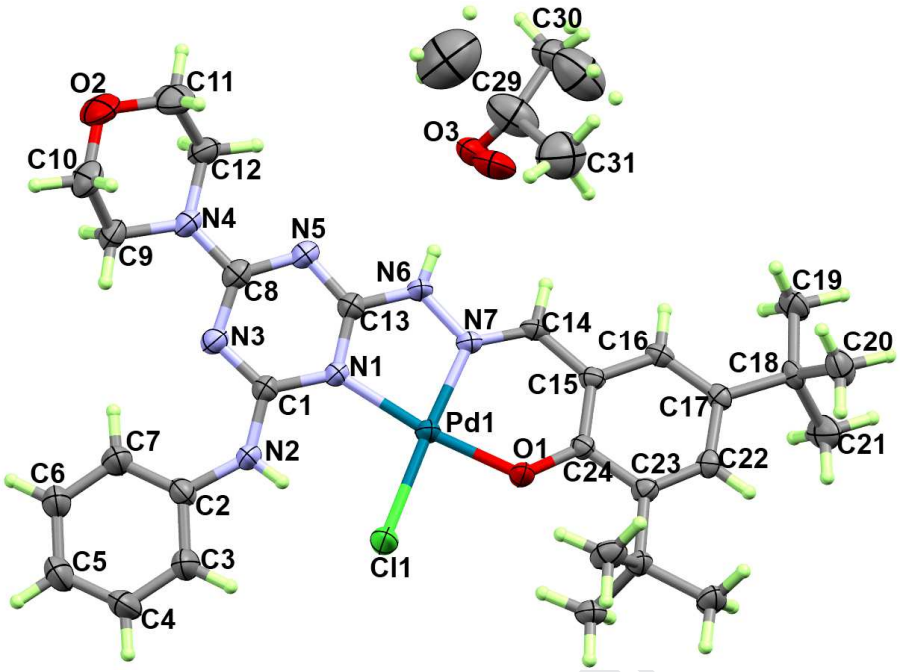

Fig. 4. X-ray structure of **[Pd(Triaz)Cl]**. Thermal ellipsoids were drawn at the 50% probability level.

Table 2. Selected bond lengths [Å] and angles [°] for **[Pd(Triaz)Cl]**.

Atoms	Distance	Atoms	Angle (°)
Pd1-N7	1.948(3)	N7-Pd1-O1	91.81(11)
Pd1-O1	1.964(2)	N7-Pd1-N1	80.78(12)
Pd1-N1	2.054(3)	O1-Pd1-N1	172.46(11)
Pd1-Cl1	2.3270(11)	N7-Pd1-Cl1	177.08(9)
		O1-Pd1-Cl1	85.27(8)
		N1-Pd1-Cl1	102.14(9)

Analysis of molecular packing

Hirshfeld d_{norm} surfaces and fingerprint plots were used to quantify the contributions of the different intermolecular interactions (**Fig. 5**). Because of the presence of a disordered solvent molecule, the Hirshfeld analysis results are presented for the two disordered components. **Fig. 6** shows a summary of the most important contacts and their contribution percentages. The two components yielded similar results; hence, the discussion was focused only on part A for simplicity. The Hirshfeld d_{norm} maps of the Pd(II) complex demonstrated that its units

are mainly packed by the nonpolar H···H interactions, which correspond to 60.6% from the whole fingerprint area. The second most abundant atom-atom interactions were the C···H contacts, accounting for 11.6%. The polar O···H, N···H, and Cl···H interactions comprised 8.1%, 3.6% and 5.0%, respectively. In Fig. 6, most of the intermolecular interactions have contact distances longer than the sum of the van der Waals radii of the two elements of each contact, except for the O···H, C···H, and C···N interactions, which appeared as red spots in the d_{norm} map (**Figs**. **7** and **8**). As shown in **Fig**. **7**, the O···H contacts is represented as an intense red circle in its d_{norm} map, indicating the hydrogen bond between the acetone oxygen atom and the proton from the N-H group of the organic ligand. According to Hirshfeld analysis, the corresponding O···H interaction distance is 1.839 Å (O3···H6); however, the refined model indicates the distance is 2.06(4) Å. The shortest C···H contacts, which belong to the C-H···π interactions, were C4···H30B and C16···H9B (2.608 and 2.696 Å). Furthermore, the shortest C···N contact was the C14···N3 (3.184 Å), indicating the existence of weak π–π stacking interactions.

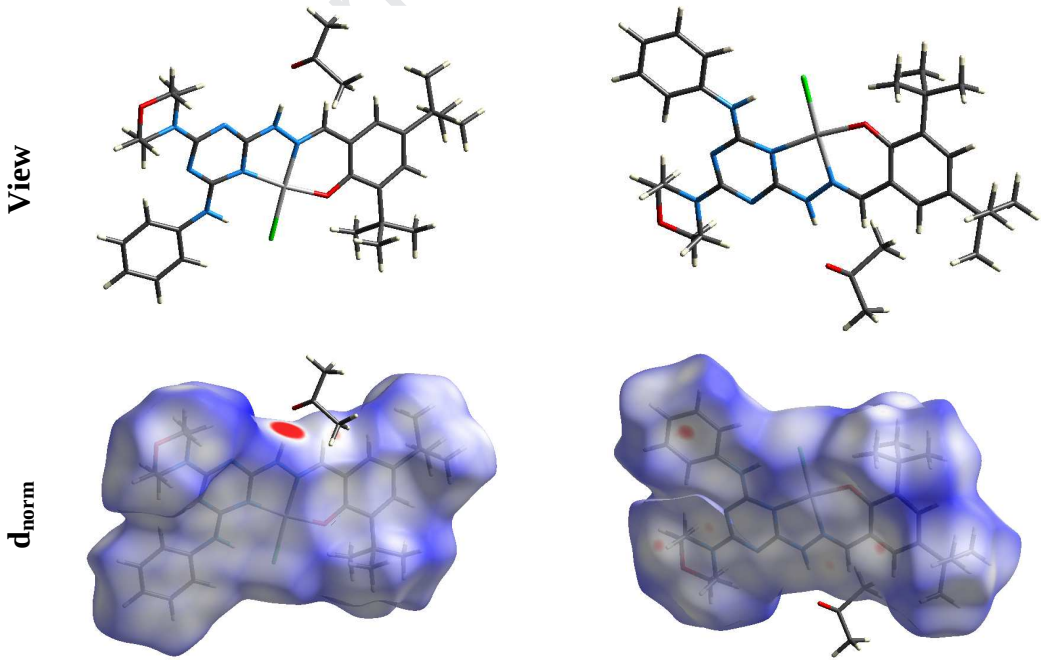

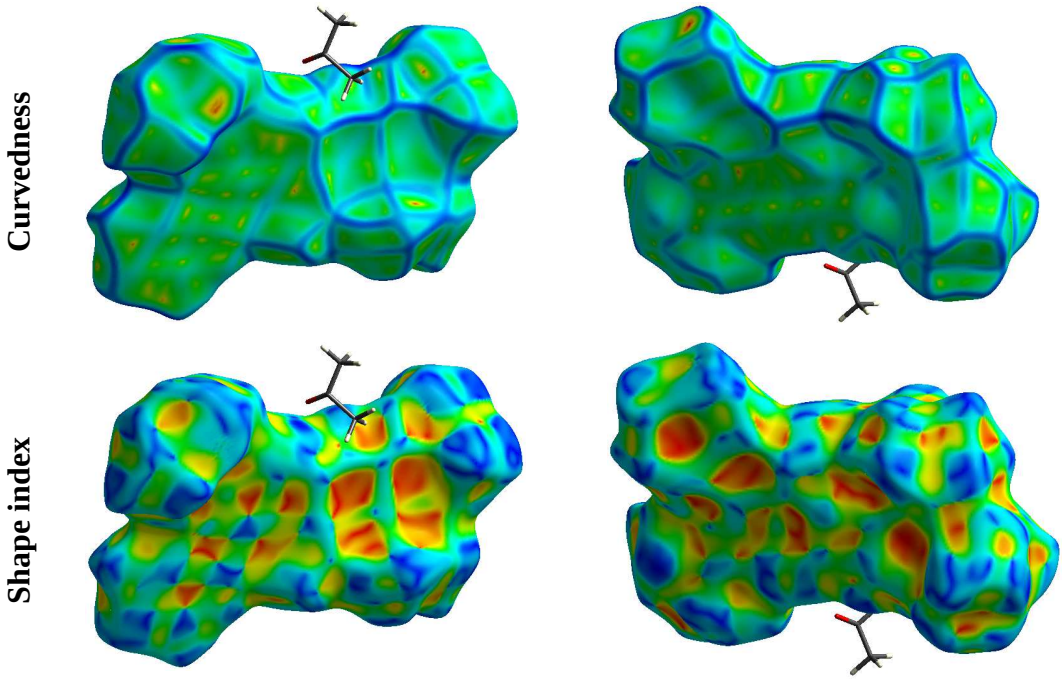

Fig. 5. Hirshfeld surfaces of the **[Pd(Triaz)Cl]** complex.

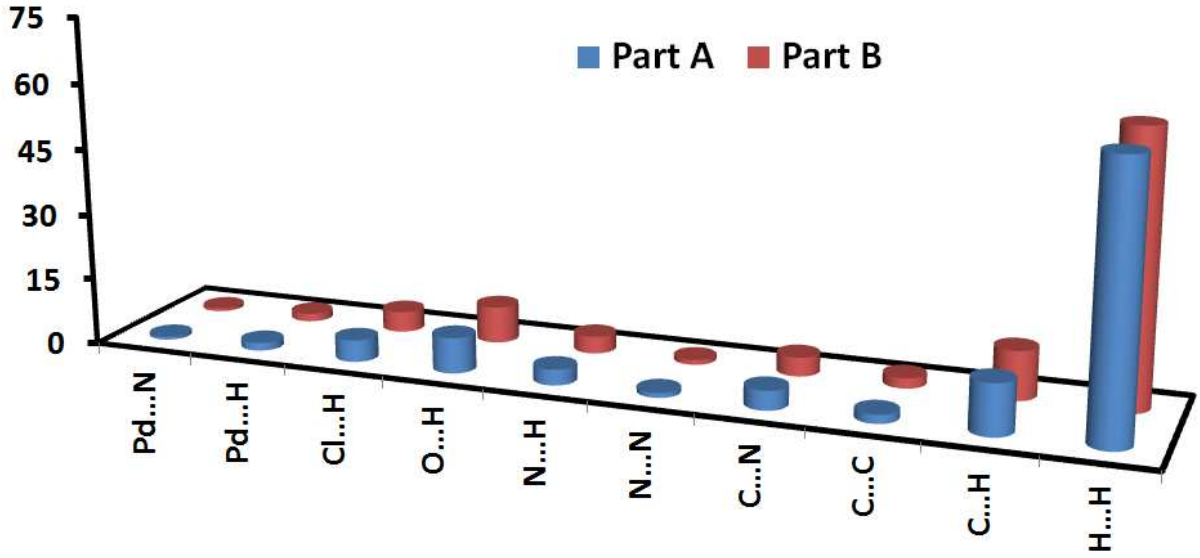

Fig. 6. Contribution percentages of the intermolecular interactions in the crystal structure of **[Pd(Triaz)Cl]**.

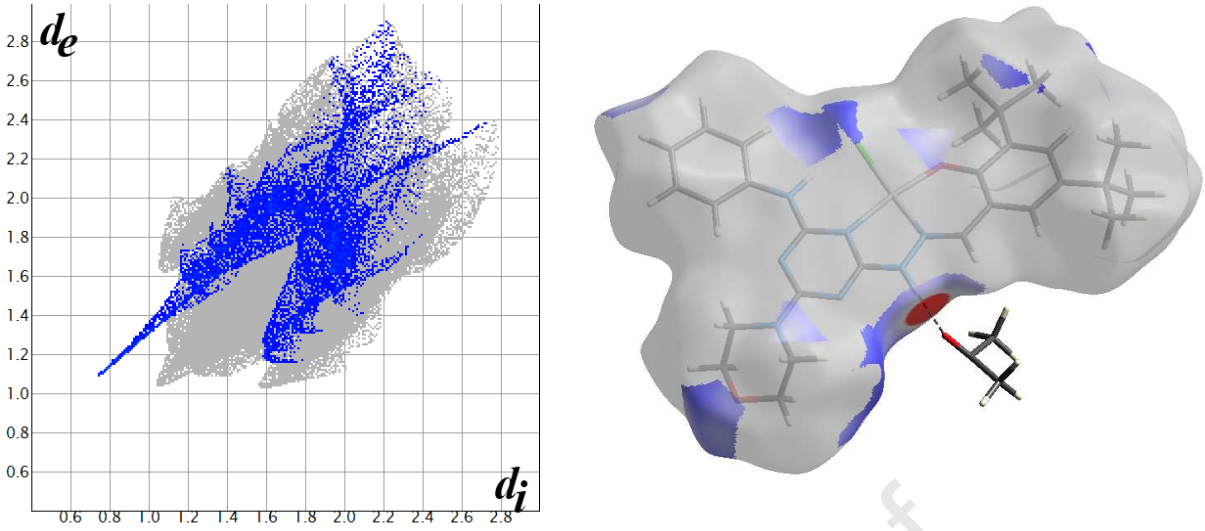

Fig. 7 2D fingerprint plot (left) and d_{norm} map (right) of the O···H contacts of**[Pd(Triaz)Cl]**.

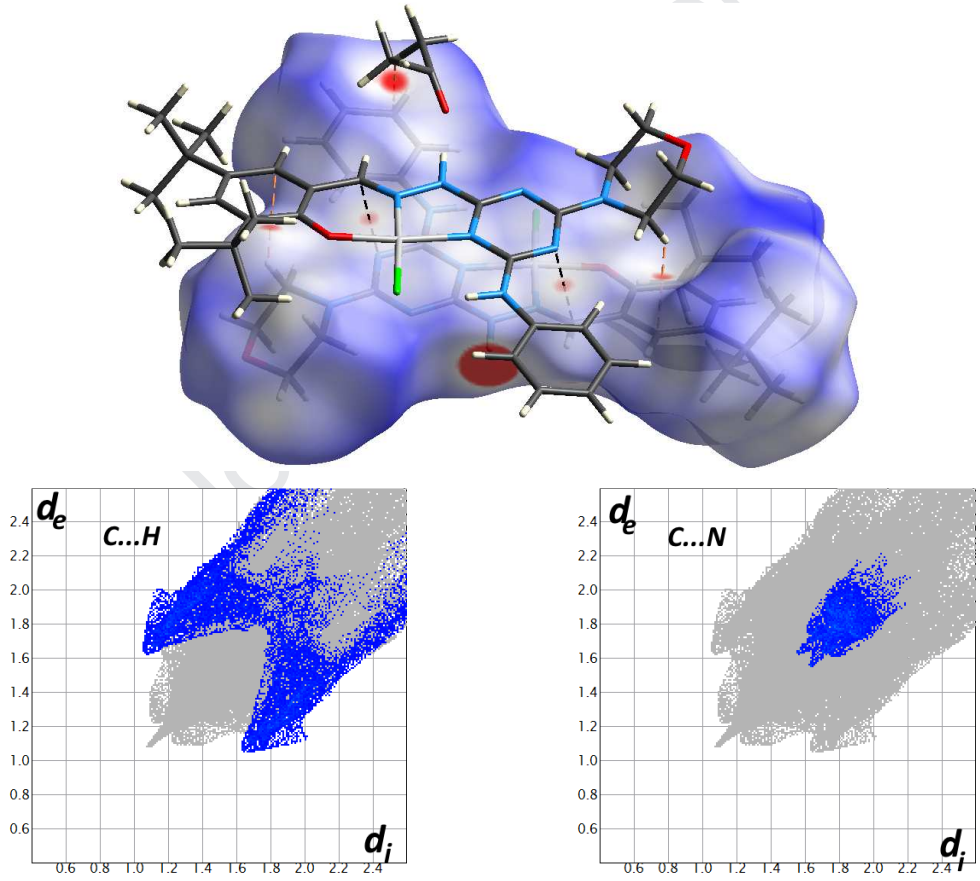

Fig. 8. Decomposed d_{norm} (−0.06 to 3.72) and FP plots of the C···H (orange) and C···N (black) contacts of **[Pd(Triaz)Cl]**.

DFT studies

Natural population analysis

The divalent Pd ion was coordinated with two negatively charged ligand groups (Cl^- and $Triaz^-$). Their charges as isolated ions were +2, −1, and −1, respectively. Because of the interaction between the Pd(II) ion (Lewis acid) and the ligand groups (Lewis bases), part of the negative charge was transferred from ligand to the Pd(II) (**Table 3**). The chloride ion transferred 0.506–0.520 e^- to Pd(II); however, the anionic organic ligand transferred almost all of its negative charge to the metal center (0.963–0.974 e^-). Therefore, $Triaz^-$ has a net charge very close to zero (−0.026 to −0.037 e^-) and the charge of Pd(II) decreased to 0.505–0.530 e^-.

Table 3. Natural charges at the Pd(II) atom, and the coordinated Cl^- and $Triaz^-$.

Atom	MPW1PW91	WB97XD
Pd	0.5053	0.5303
Cl^-	−0.4797	−0.4937
$Triaz^-$	−0.0256	−0.0367

Using natural bond orbital (NBO) calculations, the strength of the interactions between the Pd(II) center and ligand donor atoms was estimated (**Table 4**). The interaction energy of the Pd-N(hydrazone) was significantly higher than that for the Pd-N(*s*-triazine). There is only one anti-bonding natural orbital (LP*(6)) from the Pd(II) that contributes in the interaction with the N1 lone pair filled nonbonding natural orbital. The LP*(6) NBO has mainly a *s*-orbital character with some contribution from *p*-orbitals and very little contribution from *d*-orbitals. This can be inferred from the nearly spherical shape of the isodensity surface shown in **Fig. 9**. Similarly, the Pd-N(hydrazone) bonds are attributed to the interaction of the filled lone pair NBO from the corresponding nitrogen atom with the empty LP*(5)Pd anti-bonding NBO. The orbital contributions of LP*(5)Pd are very similar to LP*(6)Pd; however, the former has lesser *p*-orbital character compared to the latter. The LP*(6) NBO contributed to all of the Pd-N, Pd-O, and Pd-Cl interactions. The Pd-O coordination interaction was

attributed to the overlap between the LP(3)O filled NBO and LP*(5)Pd empty anti-bonding NBO. The net interaction energy of the Pd-O bond was 193.41 and 168.99 kcal/mol, using WB97XD and MPW1PW91 methods, respectively. The Pd-Cl coordination was attributed to the mixed interactions between the filled NBOs of the Cl^- ligand and the anti-bonding NBOs of the Pd(II) central metal ion (**Table 4**). **Fig. 9** shows the anti-bonding NBOs of Pd(II), and their corresponding occupancies and energies are listed in **Table 5**. The filled donor NBOs of the isolated ligand have almost 2.0 e^-, which are significantly lowered in the complex because of the interactions with the Pd(II) anti-bonding NBOs. The latter have almost zero occupancy in the free (isolated) Pd(II) and increased up to 0.4662 e^- in LP*(5)Pd because of the electron donation from the ligand donor atoms to the metal ion.

Table 4. The donor (**NBO_i**)-acceptor (**NBO_j**) interaction energies of Pd-N, Pd-O, and Pd-Cl coordination interactions.

NBO_i	**NBO_j**	**WB97XD**	**MPW1PW91**
LP(1)O1	LP*(5)Pd1	13.75	15.38
LP(1)O1	LP*(7)Pd1	20.41	20.00
LP(2)O1	LP*(8)Pd1	6.06	4.47
LP(3)O1	LP*(5)Pd1	116.79	97.98
LP(3)O1	LP*(6)Pd1	8.53	7.23
LP(3)O1	LP*(7)Pd1	27.87	23.93
O1→Pd1		193.41	168.99
LP(1)N7	LP*(5)Pd1	118.81	101.16
LP(1)N7	LP*(6)Pd1	11.98	10.74
LP(1)N7	LP*(7)Pd1	27.60	24.05
N7→Pd1		158.39	135.95
LP(1)N1	LP*(6)Pd1	104.23	90.88
N1→Pd1		104.23	90.88
LP(1)Cl1	LP*(5)Pd1	5.24	5.64
LP(1)Cl1	LP*(6)Pd1	4.16	4.78
LP(1)Cl1	LP*(7)Pd1	5.18	4.30
LP(2)Cl1	LP*(5)Pd1	9.63	9.38
LP(2)Cl1	LP*(6)Pd1	9.83	10.04
LP(3)Cl1	LP*(5)Pd1	1.50	1.21
LP(3)Cl1	LP*(6)Pd1	1.22	0.91
LP(3)Cl1	LP*(8)Pd1	7.17	5.68
Cl1→Pd1		43.93	41.94

Table 5. Occupancy and energy of the different NBOs included in the Pd-O, Pd-Cl, and Pd-N interactions.

	MPW1PW91		WB97XD	
NBO	**Occupancy**	**Energy**	**Occupancy**	**Energy**
LP(1)O1	1.9428	−0.5755	1.9435	−0.6305
LP(2)O1	1.7117	−0.2829	1.7186	−0.3335
LP(3)O1	1.6309	−0.4595	1.6390	−0.5106
LP(1)N1	1.6532	−0.4398	1.6604	−0.4862
LP(1)N7	1.6303	−0.4641	1.6368	−0.5104
LP(1)Cl1	1.9739	−0.4264	1.9751	−0.4851
LP(2)Cl1	1.9689	−0.7465	1.9703	−0.7951
LP(3)Cl1	1.9663	−0.2911	1.9681	−0.3683
LP*(5)Pd1	0.4662	0.0215	0.4607	0.0584
LP*(6)Pd1	0.1617	0.4265	0.1640	0.4942
LP*(7)Pd1	0.1059	0.2893	0.1075	0.3447
LP*(8)Pd1	0.0644	0.1112	0.0637	0.1653

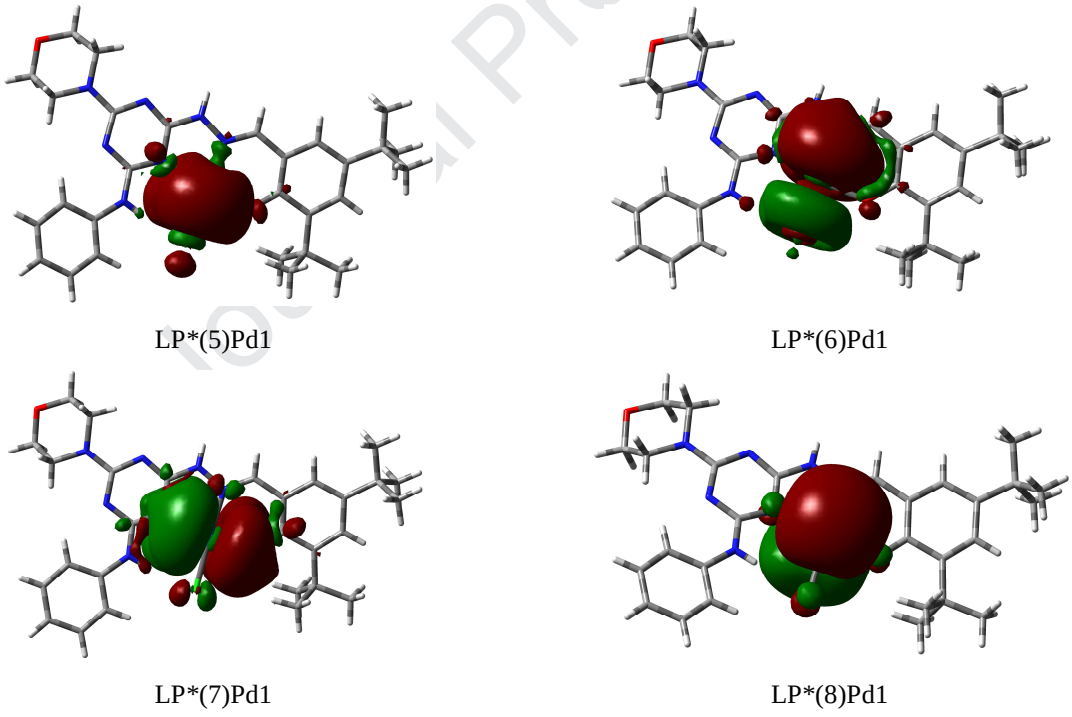

Fig. 9. Anti-bonding NBOs of Pd(II) contributing in the interactions with the NBOs of the donor ligand groups.

Antiproliferative activity

The anti-cancer activity of the synthesized metal complex **[Pd(Triaz)Cl]**, was further explored against two cancer cell lines (MCF-7 and PC3) followed by MTT assay. Initially, the cytotoxicity of starting ligand (**HTriaz**) was previously examined and reported which possess very week activity against the MCF-7 breast cancer and HCT-116 colon cancer [21]. The results shown for the antiproliferative activity of the **[Pd(Triaz)Cl]**, 18.23% inhibition against PC3 cell line at 50μg/mL. On the other hands, exhibited 7.1% inhibition when used 30μg/mL against the MCF-7 breast cancer. It can be concluded that both ligand and its Pd-(II) complex have week activity against tumor.

Conclusions

A Pd(II) complex, **[Pd(Triaz)Cl]**, with a *NNO*-donor chelate derived from hydrazono-*s*-triazine ligand was synthesized and its molecular structure investigated using different spectroscopic techniques and single-crystal X-ray diffraction combined with Hirshfeld topology analysis. The latter was performed to describe the supramolecular structure of the complex. The neutral square planar **[Pd(Triaz)Cl]** complex comprised one mono-negative tridentate ligand, $Triaz^{-}$, and one chloride ion, Cl^{-}, in the inner sphere. The O···H, C···H, and C···N interactions are the most important ones, controlling the molecular packing of the complex. DFT calculations with the aid of NBO analysis were used to describe the Pd-N, Pd-O and Pd-Cl coordination interactions. Due to the week anti-cancer activity for the metal complex and the ligand further investigation and screen for different cancer lines well be carried out in the future.

Acknowledgments

The authors would like to extend their sincere appreciation to the Deanship of Scientific Research at King Saud University for providing funding to this Research group NO (RGP −257). The authors thank the Deanship of Scientific Research and RSSU at King Saud University for their technical support.

References

1. Blotny, G. (2006). Recent applications of 2,4,6-trichloro-1,3,5-triazine and its derivatives in organic synthesis. *Tetrahedron*, *62*(41), 9507-9522.
2. Shah, D. R., Modh, R. P., Chikhalia, K. H. (2014). Privileged s-triazines: structure and pharmacological applications. *Future Med. Chem.*, *6*(4), 463-477.
3. Ramírez, J., Stadler, A. M., Brelot, L., Lehn, J. M. (2008). Coordinative, conformational and motional behaviour of triazine-based ligand strands on binding of Pb (II) cations. *Tetrahedron*, *64*(36), 8402-8410.
4. Hedayatullah, M., Lion, C., Slimane, A. B., Da Conceiçao, L., & Nachawati, I. (1999). Synthesis of reactive s-triazines bearing a cage system derived from adamantane as precursors of hexamethylmelamine analogues. *Heterocycles*, *51*(8), 1891-1896.
5. Vančo, J., Švajlenová, O., Račanská, E., Muselík, J., & Valentová, J. (2004). Antiradical activity of different copper (II) Schiff base complexes and their effect on alloxan-induced diabetes. *J. Trace Elem. Med. Bio.*, *18*(2), 155-161.
6. Jarrahpour, A., Khalili, D., De Clercq, E., Salmi, C., Brunel, J. M. (2007). Synthesis, antibacterial, antifungal and antiviral activity evaluation of some new bis-Schiff bases of isatin and their derivatives. *Molecules*, *12*(8), 1720-1730.
7. Carter, J. S., Kramer, S., Talley, J. J., Penning, T., Collins, P., Graneto, M. J., Seibert, K., Koboldt, C. M., Masferrer, J., Zweifel, B. (1999). Synthesis and activity of sulfonamide-substituted 4,5-diaryl thiazoles as selective cyclooxygenase-2 inhibitors. *Bioorg. Med. Chem. Lett.*, *9*(8), 1171-1174.
8. Kolesinska, B., Kaminski, Z. J. (2009). The Umpolung of substituent effect in nucleophilic aromatic substitution. A new approach to the synthesis of N,N-disubstituted melamines (triazine triskelions) under mild reaction conditions. *Tetrahedron*, *65*(18), 3573-3576.
9. Khattab, S. N., Khalil, H. H., Bekhit, A. A., Abd El-Rahman, M. M., de la Torre, B. G., El-Faham, A., Albericio, F. (2018). 1,3,5-Triazino peptide derivatives: synthesis, characterization, and preliminary antileishmanial activity. *ChemMedChem*, *13*(7), 725-735.
10. Sunduru, N., Gupta, L., Chaturvedi, V., Dwivedi, R., Sinha, S., Chauhan, P. M. (2010). Discovery of new 1,3,5-triazine scaffolds with potent activity against Mycobacterium tuberculosis H37Rv. *Eur. J. Med. Chem.*, *45*(8), 3335-3345.

11. Zhou, C., Min, J., Liu, Z., Young, A., Deshazer, H., Gao, T., Chang, T., Kallenbach, N. R. (2008). Synthesis and biological evaluation of novel 1,3,5-triazine derivatives as antimicrobial agents. *Bioorg. Med. Chem. Lett.*, *18*(4), 1308-1311.
12. Sosič, I., Mirković, B., Turk, S., Štefane, B., Kos, J., Gobec, S. (2011). Discovery and kinetic evaluation of 6-substituted 4-benzylthio-1,3,5-triazin-2 (1H)-ones as inhibitors of cathepsin B. *Eur. J. Med. Chem.*, *46*(9), 4648-4656.
13. Garaj, V., Puccetti, L., Fasolis, G., Winum, J. Y., Montero, J. L., Scozzafava, A., Vullo, D., Innocenti, A., Supuran, C. T. (2005). Carbonic anhydrase inhibitors: novel sulfonamides incorporating 1,3,5-triazine moieties as inhibitors of the cytosolic and tumour-associated carbonic anhydrase isozymes I, II and IX. *Bioorg. Med. Chem. Lett.*, *15*(12), 3102-3108.
14. Bai, F., Liu, H., Tong, L., Zhou, W., Liu, L., Zhao, Z., Liu, X., Jiang, H., Wang, X., Xie, H., & Li, H. (2012). Discovery of novel selective inhibitors for EGFR-T790M/L858R. *Bioorg. Med. Chem. Lett.*, *22*(3), 1365-1370.
15. El-Faham, A., Soliman, S. M., Ghabbour, H. A., Elnakady, Y. A., Mohaya, T. A., Siddiqui, M. R., Albericio, F. (2016). Ultrasonic promoted synthesis of novel s-triazine-Schiff base derivatives; molecular structure, spectroscopic studies and their preliminary anti-proliferative activities. *J. Mol. Struct.*, *1125*, 121-135.
16. Menear, K. A., Gomez, S., Malagu, K., Bailey, C., Blackburn, K., Cockcroft, X. L., Ewen, S., Fundo, A., Le Gall, A., Hermann, G., Sebastian, L., (2009). Identification and optimisation of novel and selective small molecular weight kinase inhibitors of mTOR. *Bioorg. Med. Chem. Lett.*, *19*(20), 5898-5901.
17. Soliman, S. M., El-Faham, A. (2019). Synthesis and structural DFT studies of Ni (II) and Co (II) complexes with s-triazine-based di-compartmental ligand. *Polyhedron*, *165*, 162-170.
18. Soliman, S. M., El-Faham, A. (2019). Synthesis, molecular structure and DFT studies of two heteroleptic nickel (II) s-triazine pincer type complexes. *J. Mol. Struct.*, *1185*, 461-468.
19. a) Soliman, S. M., El-Faham, A. (2019). Synthesis and structure diversity of high coordination number Cd (II) complexes of large s-triazine bis-Schiff base pincer chelate. *Inorg. Chim. Acta*, *488*, 131-140 and b) Soliman, S. M., & El-Faham, A. (2018). Synthesis, characterization, and structural studies of two heteroleptic Mn (II) complexes with tridentate N,N,N-pincer type ligand. *J. Coord. Chem.*, *71*(15), 2373-2388.

20. a) Zhang, A., Xu, L., Lei, G. (2016). Separation and complexation of palladium(II) with a new soft N-donor ligand 6,6′-bis(5,6-dinonyl-1,2,4-triazin-3-yl)-2,2′-bipyridine (C9-BTBP) in nitric acid medium, *New J. Chem.*, *40*, 6374-6383; b) Xu, L., Zhang, A., Pu, N., Lu, Y., Yang, H., Liu, Z., Ji, Y. (2019). Unusual complexation behaviors of R-BTPs with water molecule and Pd(II) caused by electronic modulation of substituents on BTP backbone: new insights into palladium separation under the framework of minor actinides' partitioning, *New J. Chem.*, *43*, 9052-9065; c) Xu, L., Zhang, A., Pu, N., Xu, C., Chen, J. (2019). Preparation and characterization of a novel macroporous silica-bipyridine asymmetric multidentate functional adsorbent and its application for heavy metal palladium removal, *J. Hazard. Mat.*, *376*, 188-199; d) Xu, L., Zhang, A., Lu, Y., Yang, H. & Liu, Z. A. (2016). Phenanthroline-derived ligand and its complexation with Pd(II): from ligand design, synthesis and Pd(II) complexes structures to its application, *RSC Adv*, *6*, 99859-99866; e) Zhang, A., Wang, X. , Chai, Z. (2010). Synthesis of a macroporous silica-based derivative of pyridine material and its application in separation of palladium, *AICHE Journal*, *56*(12), 3074-3083.
21. Barakat, A., El-Senduny, F. F., Almarhoon, Z., Al-Rasheed, H. H., Badria, F. A., Al-Majid, A. M., Ghabbour, H. A., El-Faham, A. (2019). Synthesis, X-ray crystal structures, and preliminary antiproliferative activities of new s-triazine-hydroxybenzylidene hydrazone derivatives. *Journal of Chemistry*, *2019* Article ID 9403908, 10.
22. Otwinowski, Z., Minor, W. Processing of X-ray Diffraction Data Collected in Oscillation Mode, Academic Press, New York, pp. 307-326, 1997. In *Methods in Enzymology, Volume 276, Macromolecular Crystallography, Part A*, Carter, C. W., Sweet, J., Eds.; Academic Press: New York, USA, 1997; pp 307-326.
23. Sheldrick, G. M. *SADABS - Bruker Nonius scaling and absorption correction* -, Bruker AXS, Inc.: Madison, Wisconsin, USA, 2012.
24. Sheldrick, G. M. (2015). Crystal structure refinement with SHELXL. *Acta Crystallogr. C*, C71, 3-8.
25. Hübschle, C. B., Sheldrick, G. M. Dittrich, B. (2011). ShelXle: a Qt graphical user interface for SHELXL. *J. Appl. Cryst. 44*, 1281-1284.
26. Turner, M. J., McKinnon, J. J., Wolff, S. K., Grimwood, D. J., Spackman, P. R., Jayatilaka, D., & Spackman, M. A. Crystal Explorer17 (2017) University of Western Australia. http://hirshfeldsurface.net.

27. Frisch, M.J., Trucks, G.W., Schlegel, H.B., Scuseria, G.E., Robb, M.A. et al., (2009) Gaussian, Inc., Wallingford CT, 2009.

28. a) Chai, J. D. & Head-Gordon, M. (2008). Long-range corrected hybrid density functionals with damped atom–atom disperson corrections. *Phys. Chem. Chem. Phys.*, *10*, 6615; b) Adamo C., Barone, V. (1998). Exchange functionals with improved long-range behavior and adiabatic connection methods without adjustable parameters: The mPW and mPW1PW models, *J. Chem. Phys.*, *108*, 664-75.

29. a) https://bse.pnl.gov/bse/portal; b) Feller, D. (1996). The role of databases in support of computational chemistry calculations. *J. Comp. Chem.*, *17*, 1571-1586; c) Schuchardt, K. L., Didier, B.T., Elsethagen, T., Sun, L., Gurumoorthi, V., Chase, J., Li, J., & Windus, T. L. (2007). Basis set exchange: A community database for computational sciences, *J. Chem. Inf. Model.*, *47*,1045-1052.

30. NBO Version 3.1, E.D. Glendening, A.E. Reed, J.E. Carpenter, F. Weinhold, NBO Version 3.1, CI, University of Wisconsin, Madison, 1998.

Highlights

- The new Pd(II) complex **[Pd(Triaz)Cl]** bearing hydrazono-*s*-triazine ligand explored.
- The molecular structure assigned by X-ray single crystal technique.
- Molecular insights were also investigated.

author statement

Saied M. Soliman, Jamal Lasri, and Assem Barakat: Conceptualization, Supervision, **Jamal Lasri, and Assem Barakat:** Investigation, Methodology, **Saied M. Soliman and Matti Haukka**: Data curation, Writing- Original draft preparation. **Adel Elmarghany, Abdullah Mohammed Al-Majid, Ayman El-Faham**: Visualization, Validation.**: Saied M. Soliman,** and **Matti Haukka**: Software, Validation.: **All:** Writing- Reviewing and Editing, Approval the final manuscript.

Conflicts of Interest

"The authors declare no conflict of interest."